

# Particle Path Tracking Method in RDE

Rui Zhou Jian-ping Wang

Dept. of Mechanics and Aerospace Engineering/State Key Lab. Of Turbulence and Complex Systems, College of Engineering, Peking University  
Beijing, China, 100871

## 1 Introduction

In recent years, the rotating detonation engine (RDE) based on detonation combustion has been extensively studied [1-5]. So far, there has been little research, by both numerical simulations and experiments, of the thermodynamic performance of the RDE. In the previous work, We have proposed the particle path tracking method to analyze the two-dimensional RDE flow field and describe its thermodynamic properties [6]. The paths of flow particles are tracked, and the effects of the detonation wave, the deflagration wave, the oblique shock wave and the contact surface on the paths and flow parameters are investigated. The corresponding p-v and T-s diagrams can then be used to calculate the net mechanical work and thermal efficiency. The results from numerical simulations are qualitatively and quantitatively compared with the ideal ZND model.

In this paper, the particle path tracking method is further applied in the 2D and the 3D RDE numerical simulation. We focus on the movement of the flow particles in the 3D RDE combustion chamber, and the comparative analysis of the paths and the thermodynamic cycle processes between the 2D and the 3D numerical simulation. The paths of flow particles are tracked in the 2D and the 3D combustion chamber, and the effects of the several waves in the RDE flow field on the paths are investigated. The corresponding p-v and T-s diagrams obtained by the 3D numerical simulation are consistent with that obtained by the 2D numerical simulation.

In the 2D and the 3D numerical simulation, the flow field is governed by the conservation Euler equations and Korobeinikov [7] two-step chemical reaction model. The viscosity, thermal conduction and mass diffusion are ignored. The parameters in equations are selected to agree with [7] and [8]. Spatial terms are discretized with 5th order WENO scheme[9], and temporal terms are discretized with 4-steps Runge-Kutta method[10].

The entire flow field is initially filled with the premixed stoichiometric hydrogen and oxygen mixture at 1 atm and 300 K, except near the head wall region where an azimuthally propagating C-J detonation wave is artificially placed to initiate 2D and 3D detonations. The inlet total pressure is 3 MPa. At the head end, there are a large number of Laval micro-nozzles to axially inject premixed stoichiometric hydrogen/oxygen gas into the combustion chamber. The mass flux of the incoming fuel is controlled by the relationship between the inlet stagnation pressure and the flow pressures at the head end. At the exit plane, we use Non-reflecting outlet boundary condition. The radius of the 2D combustion chamber is 4.5 cm, and the length is 4.8cm. The inner radius of the 3D combustion

chamber is 4 cm, length 4.8 cm, and the chamber width is 1 cm. The regular grid size used is 0.2 mm, whose dependency has been validated in [11].

## 2 2D paths Analysis

In the two-dimensional numerical simulation, we ignore the chamber width along the radial direction, therefore the flow field can be approximated as a 2D cylindrical chamber without thickness. Figure 1 shows the distribution of the reaction process variable after the detonation propagates in a stable manner. The initial positions of the tracked particles are marked 1, 2, ..., 8 in Fig. 1. Particles 1-7 are burned by the detonation wave, and particle 8 is burned by the deflagration wave between the fresh gas and the combustion product. Figure 2 shows the paths of the eight particles from injection into the combustion chamber to exhaustion. It is seen that the paths are generally along the axial direction no matter where their initial positions are. The particle paths have small fluctuations in the azimuthal direction, and the fluctuation of particle 2 is maximum, which is only 8.3% of the circumference of the combustion chamber. Flow particles are injected into the combustion chamber, burned by the detonation wave or the deflagration wave, and then rapidly ejected almost along the axial direction. This character supports that a RDE can produce the axial thrust.

Particles 1-7 encounter the detonation wave, and at this instant their paths are deflected, as shown the intersection points among the paths and the line of detonation wave (DL) in Fig.2. The path of particle 8 is not deflected when it encounters the deflagration wave. Particle 1 and particle 8 encounter the attached oblique shock wave and their paths are deflected again, as shown the intersection points among the paths and the line of the shock wave in Fig. 2. More detailed description is shown in [3].

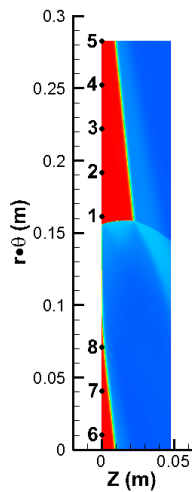


Figure 1. Reaction process variable contour and initial positions of the tracked particles.

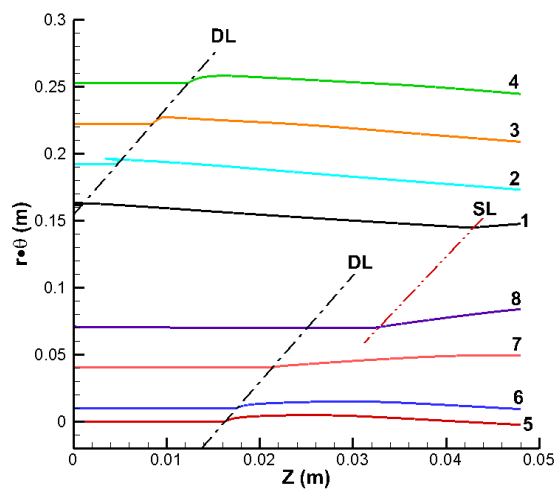


Figure 2. Paths of eight particles.

## 3 3D paths Analysis

Figure 3 shows the pressure contour in the 3D RDE combustion chamber after the detonation propagates dynamically stable. A detonation wave propagates azimuthally in the annular chamber while a combustible mixture is injected from the head end, and the burnt gas then flows out from the downstream exit.

The initial positions of the tracked particles are shown in Fig.4, which are different along the azimuthal direction and the radial direction. Figure 5 shows the paths fluctuations along the azimuthal direction of the flow particles, whose initial positions are on the middle annulus. Eight particles all encounter the detonation wave after they are injected into the combustion chamber, and at this instant their paths are deflected, as shown the intersection points among the paths and the line DL in Fig.5. Due to the short length of the combustion chamber in the numerical simulation, the particles flow out

from the combustion chamber so rapidly that they have not encountered the oblique shock wave attached after the detonation wave. Therefore the paths have not been deflected again. The path fluctuation along the azimuthal direction is very small like the 2D paths, and the fluctuation of particle 11 is maximum, which is only 8.7% of the circumference of the middle annulus.

Figure 6 shows the variation of particle 1's path, pressure and temperature with the axial distance. Particle's pressure and temperature increase rapidly, and its path is deflected when it encounters the detonation wave. After encountering the detonation wave, the pressure decreases rapidly until it is increased suddenly because of the reflected shock wave after the detonation wave.

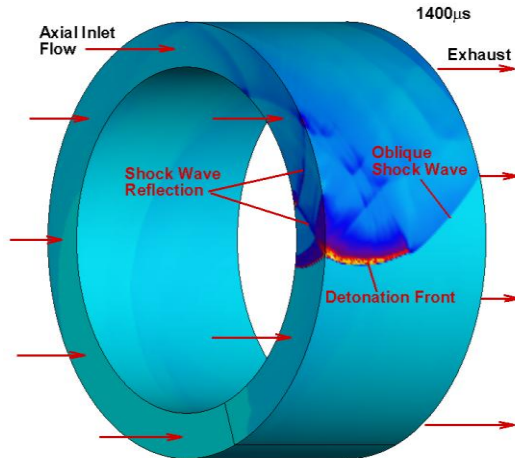


Figure 3. Pressure contour.

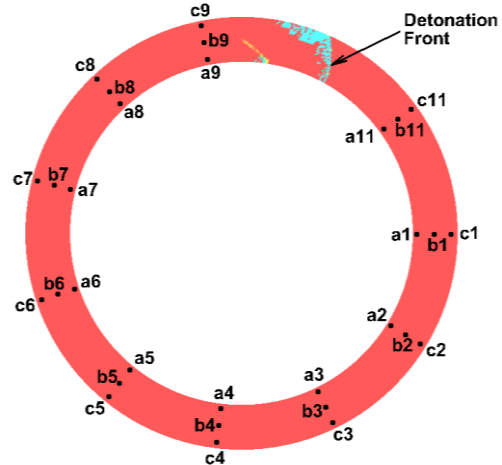


Figure 4. Initial positions of tracked particles.

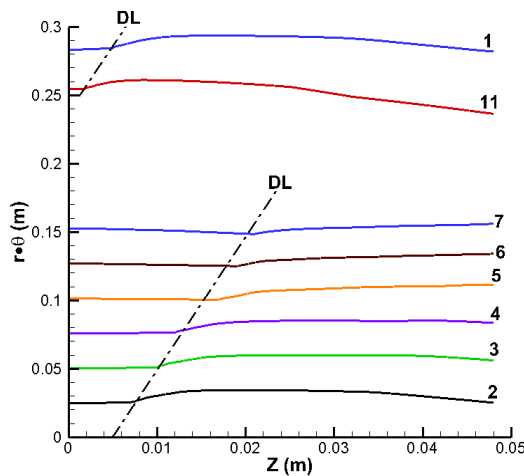


Figure 5. Paths of particles on the middle annulus.

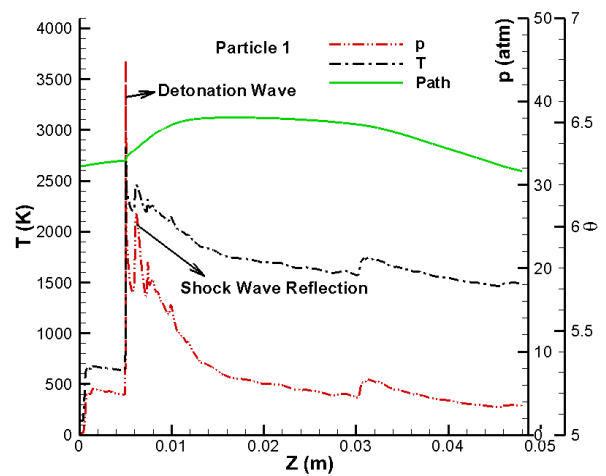


Figure 6. Path, pressure and temperature of particle 1.

Now we analyze the paths of the particles in detail, whose initial positions are different along radial direction. Figure 7 and 8 show the paths along the azimuthal direction and the radial direction as time variable, whose initial positions are marked a1, b1 and c1 in Fig.4. The paths variations along the azimuthal direction of the three particles, whose initial positions are on the inner, middle and outer annulus respectively, are almost the same. They are deflected when they encounter the detonation wave, and the three particles do not encounter the oblique shock wave. The paths fluctuations along the radial direction are not obvious, as shown in Fig. 8. The detonation wave near the concave wall is convergent and therefore stronger than that near the divergent convex wall. The velocities along axial direction of the particles decrease rapidly when they go through the detonation wave, and the stronger detonation wave lead to the more degree reduce of the axial velocity. Figure 9 shows the axial velocity of the particle on the outer annulus is smaller than that on the inner annulus. The particle, whose initial position is on the outer annulus, needs longer time to flow out from the combustion chamber than that

on the middle and inner annulus. Figure 8 shows the outer the particle's position is, the bigger its path fluctuation along the radial direction is. The reason for that is that both the detonation wave and the reflected shock waves are stronger on the outer annulus than that on the inner annulus.

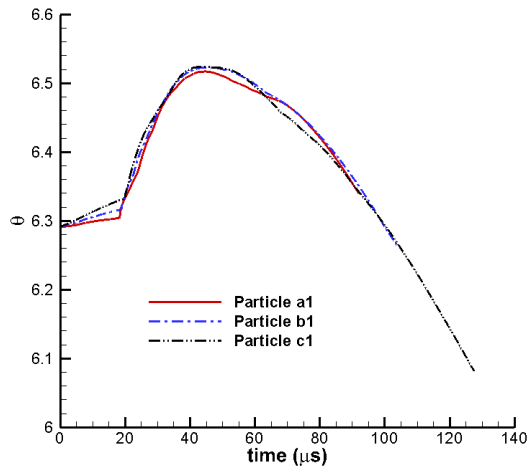


Figure 7. Paths along azimuthal direction.

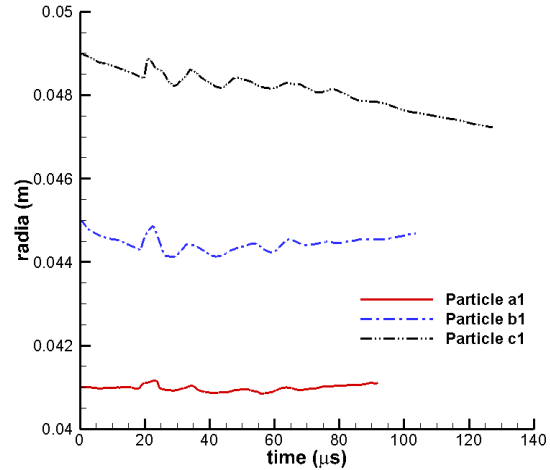


Figure 8. Paths along radial direction.

## 4 Comparison of 2D and 3D Results

Figure 10 shows the paths comparison of the particle 3 in the 2D numerical simulation and the particle 1 in the 3D numerical simulation. The fluctuant trend along the azimuthal direction of the 3D path is coincident with the 2D path, however the deflection of the 3D path is more gentle than the 2D path. The paths both deflect when the particles encounter the detonation wave.

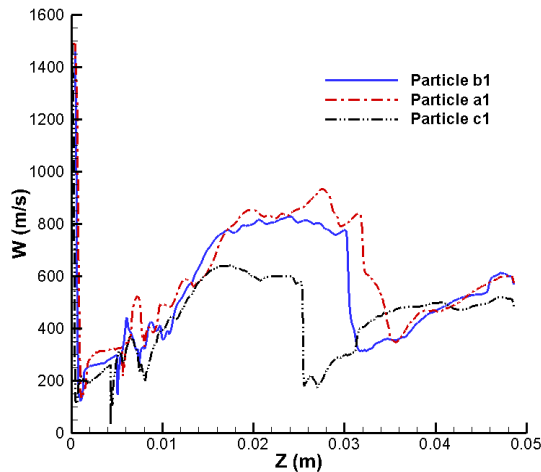


Figure 9. Axial velocity of the three particles initial positions on the inner, middle and outer annulus.

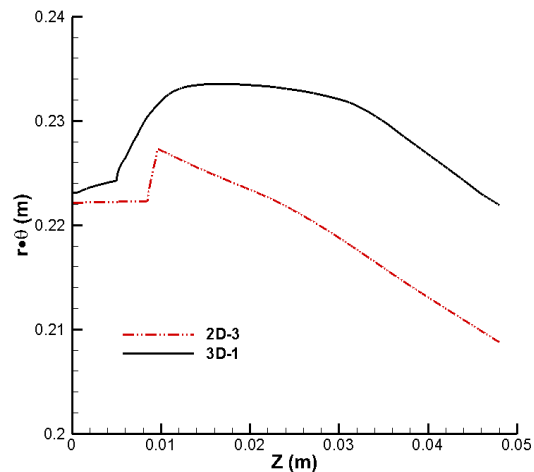


Figure 10. Paths comparison of 2D and 3D numerical simulations.

Pressure as a function of specific volume is defined by the p-v diagram, which represents the mechanical work of the thermodynamic processes. Temperature as a function of the entropy increment is defined by the T-s diagram, which represents the heat release of the thermodynamic processes. In this paper, the p-v and T-s diagrams of the 3D and the 2D RDE are shown in Fig.11. The p-v and T-s diagrams obtained by the 3D numerical simulation are consistent with the 2D numerical simulation. The p-v diagrams show the detonation combustion is similar to the constant-volume combustion, and the T-s diagrams show the expansion process is similar to the isentropic expansion. The 3D detonation wave are more complex than the 2D detonation wave. The transverse waves only exist in the axial direction in the 2D detonation flow field, however the transverse waves exist both in the axial and the radial directions in the 3D detonation flow field. Therefore the maximum pressure in the 3D p-v

diagram is higher than that in the 2D p-v diagram, and the entropy increment in the 3D T-s diagram is slightly smaller than the 2D T-s diagram. We also know from the Fig.11 that the net mechanical work and the thermal efficiency of the cycle obtained by the 3D numerical simulation are similar to the 2D results.

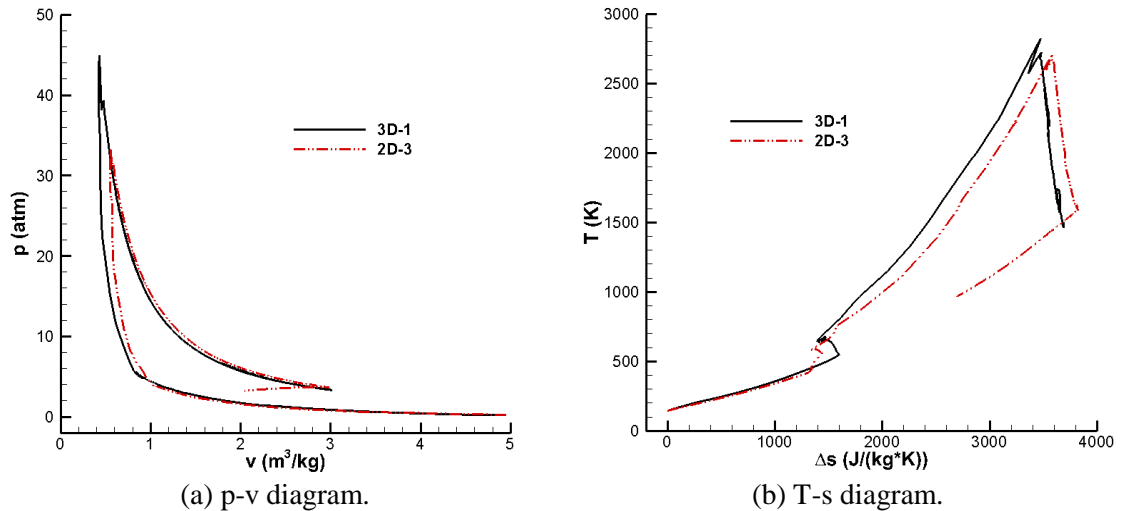


Figure 11. Comparison of the p-v and T-s diagrams from 2D numerical simulation and 3D numerical simulations.

## 5 Conclusions

(1) In the 2D and the 3D RDE flow field, the paths of the flow particles only have a small fluctuation in the azimuthal direction. Flow particles are injected into the combustion chamber, burned by the detonation wave or the deflagration wave, and then rapidly ejected almost along the axial direction. When the flow particles encounter the detonation wave or the oblique shock wave, their paths are deflected. When the flow particles encounter the deflagration wave or the contact surface, their paths are not deflected.

(2) The fluctuant trend along the azimuthal direction of the 3D path is coincident with the 2D path, however the deflection of the 3D path is more gentle than the 2D path.

(3) The p-v and T-s diagrams obtained by the 3D numerical simulation are consistent with the 2D numerical simulation, and the net mechanical work and the thermal efficiency of the cycle obtained by the 3D numerical simulation are similar to the 2D results. The p-v diagrams show the detonation combustion is similar to the constant-volume combustion, and the T-s diagrams show the expansion process is similar to the isentropic expansion. The maximum pressure in the 3D p-v diagram is higher than that in the 2D p-v diagram, and the entropy increment in the 3D T-s diagram is slightly smaller than the 2D T-s diagram.

## References

- [1] Tae-Hyeong Yi, Jing Lou, Cary Turangan, Choi, J.Y., Wolanski, P. (2011). Propulsive performance of a continuously rotating detonation engine. *Journal of Propulsion and Power* 27(1): 171-181.
- [2] Kindracki, J., Wolanski, P., Gut, Z. (2011). Experimental research on the rotating detonation in gaseous fuels-oxygen mixtures. *Shock Waves* 21: 75-84.
- [3] Bykovskii F. A., Zhdan S. A., Vedernikov E. F.(2006). Continuous spin detonation. *Journal of propulsion and power* 22(6): 1204-1216.

- 
- [4] Hishida M., Fujiwara T., Wolanski P.(2009). Fundamentals of rotating detonation. Shock waves 19 (1): 1-10.
  - [5] Yuho Uemura, A. Koichi Hayashi, Makoto Asahara, Nobuyuki Tsuboi, Eisuke Yamada.(2013) Transverse wave generation mechanism in rotating detonation. Proceedings of the Combustion Institute 34 (2): 1981-1989.
  - [6] Zhou Rui, Wang Jian-Ping. (2012). Numerical investigation of flow particle paths and thermodynamic performance of continuously rotating detonation engines. Combustion and Flame 159: 3632-3645.
  - [7] Korobeinikov V. P., Levin V. A. (1972). Propagation of blast waves in a combustible gas [J]. Astronautica Acta 17(4-5): 529-537.
  - [8] Bussing, T R A.Hinkey J. B.(1994). Pulse Detonation Engine Preliminary Design Considerations. AIAA paper 94-3220.
  - [9] Liu X. D., Osher S. and Chan T.(1994). Weighted essentially non-oscillatory shock-capturing scheme. Journal of Computational Physics 115: 200-212.
  - [10] Shu C.W. and Osher S.(1989). Efficient Implementation of Essentially Non-Oscillatory Shock-Capturing Schemes II. J. Comp.Phys. 83: 32-78.
  - [11] Shao Y.T., Wang J.P. (2010). Continuous Detonation Engine and Effects of Different Types of Nozzle on Its Propulsion Performance. Chinese Journal of Aeronautics 23(6): 647-652.